Mon. Not. R. Astron. Soc. **000**, ??–?? (2011) Printed 14 November 2011 (MN LATEX style file v2.2)

A Spatial FFT and FX Correlator for the BEST-2 Array

G. Foster[1], J. Hickish[1], D. Price[1], K. Zarb Adami[1]
[1] *Oxford University, Department of Physics*

14 November 2011

ABSTRACT
A new FX correlator and a spatial FFT imager has been developed using CASPER FPGA hardware for the BEST-2 array at the Radiotelescopi di Medicina in Italy. Both instruments use the same digitizing/channelizing front end. The spatial FFT imager takes advantage of BEST-2 as a regularly gridded array to perform a 2D spatial FFT using $O(n \log n)$ operations. The FX correlator has been used to solve complex gain calibrations which are applied in the spatial FFT during observation. During the initial deployment of the instruments several bright radio sources were observed over multiple epochs.

1 INTRODUCTION

The BEST-2 test bed at the Radiotelescopi di Medicina in Italy has been extended with a new digital backend. This digital backend consists of a 32 element digitizer, FX correlator, spatial FFT imager and beamformer implimented on ROACH FPGA boards. The Basic Element for SKA Training (BEST) test beds, consisting of BEST-1, BEST-2, and BEST-3lo, were developed as prototype systems for SKA hardware development. Simplicity of interfacing with different digital backends was a core component of each design. Digital firmware development was designed and tested at Oxford and the designs transfered with minimal changes to the available hardware at Medicina. A digital backend was installed during the initial setup of BEST-2 using a previous generation of CASPER FPGA hardware (). This new backend implimenets the same FX correlator functionality but also provides a high speed 10 GbE output interface for millisecond resolution correlations. Along with the correlator a spatial fast Fourier Transform (FFT) imager is incorporated which uses the antenna array grid layout to perform a spatial transform to produce a uniform grid of beams covering the array field of view. The imager also has a selectable 10 GbE beam output with can be used with a pulsar processor. These instruments have been installed as prototypes for larger scale instruments currently in development. The correlator is beinging used to study the handling of large output data rates and the development of real time millisecond imaging using many antenna elements. The feasablitiy and limitations of the spatial FFT imagger is not well understood. Design and deployment of a prototype design is key to understanding the possible future uses for such an instrument. We have successfully observed a number of sources with the correlator and imager over the deployment period. Data has been reduced and calibrated using a combination of custom software and standard radio synthesis imaging packages.

1.1 BEST-2 Array

The BEST-2 testbed at the Medicina Radio Observatory consists of 32 recievers on 8 cylindrical concetrators which make up a portion of the North Cross array. The array is laid out on a *4-by-8* grid, fig. 1, this makes it possible to perform the spatial FFT transform. This system was developed as a reliable, low cost develpment backend (Montebugnoli 2009). The array has an effective collecting area of approximately 1000 m^2 and covers a 16 MHz band centered at 408 MHz. The longest North-South baseline is 70 m and East-West 17 m for a synthesized beam of 0.9° square at 408 MHz. Further specifications of the array characteristics have been listed in table 1. Exstensive documentation and development of the analogue chain can be found in a number of papers (Perini 2009) (Perini 2009). In 2008 the initial digital correlator backend of the array was based on iBOB and BEE2 FPGA boards from the Collaboration for Astronomy Signal Processing and Electronics Research (CASPER)(Montebugnoli 2009). An upgraded digital backend has been developed using the ROACH board, also developed by CASPER, which includes an FX correlator, spatial FFT imager and beamformer.

BEST-2 Array Specifications		
Cylinder Properties		
Number of RX per Cylinder	4	
Cylinder Diameter	7.5	m
Cylinder Lenght	23.5	m
Element Diameter	7.5	m
Element Lenght	5.88	m
Element Collecting Area	44.1	m^2
Aperture Efficiency	0.71	
Element Effective Area	31.311	m^2
BEST-2		
Number of Cylinders	8	
Total Number of RX	32	
Total Collective Area	1411.2	m^2
Total Effective Area	1001.95	m^2
Sensitivity / Ant. gain	0.36	K/Jy
A_{eff}/T_{sys}	11.65	m^2/K
Antenna Temperature	35	K
Receiver Temperature	51	K
System Temperature	86	K
Longest Baseline		
E-W	17.04	m
N-S	70.00	m
Bandpass		
Central Frequency	408	MHz
Analog Bandwidth	16	MHz
Pointing Limits		
Declination	(0,+90)	deg
Right Ascension	Local Meridian	
Primary Beam		
Primary Beam Size	37.62	deg^2
Declination	5.7	deg
Right Ascension	6.6	deg
PSF		
PSF FWHM	0.9	deg^2
Declination	0.52	deg
Right ascension	1.73	deg

Table 1. The North Cross array is a transitting array, a section of the North-South arm was upgraded in 2008 as BEST-2.

2 INSTRUMENT DESIGN

An FX correlator and spatial FFT imager instrument have been built for BEST-2. Both instruments use the same digitization and channelization frontend. This allow a streamlined process of calibrating the spatial FFT imager, reduces the amount of hardware and allows for simultaneous observation with both instruments. The instrument has been implemeneted on ROACH boards which are a generic field programmable gate array (FPGA) board designed by CASPER for radio astronomy applications. A ROACH consits of a XILINX Virtex 5 SX95T FPGA with interfaces to DRAM and QDR memory, high speed CX-4 connectors and a generic Z-DOK interface for connecting ADCs and various daughter boards, fig 2. Additionally, the board has a PowerPC running BORPH, a variant of Debian Linux, which allows access to software registers and shared

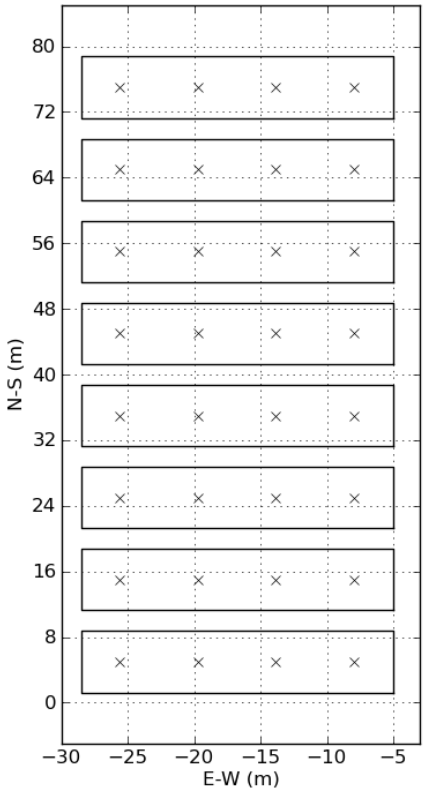

Figure 1. Each cylinder has 64 dipoles, 16 dipoles are analog beamformed to create four independent receivers.

memory on the FPGA. Firmware is designed using MATLAB Simulink which is extended with XILINX DSP blocks and CASPER's open source DSP blocks(). Design specific DSP blocks and hardware interfaces have also created, design models and control software are available from our project repository(). Instrument design specifications are presented in table 2, further design detail is described in the following sections.

2.1 Digitization and Channelization

Signal digitization is performed using the Texas Instruments ADS5272 8 channel, 12 bit ADC. The ADC board, developed by Rick Raffanti (), uses eight of these ADCs to channelize 64 streams at up to 65 Msps. In our design only 32 signal streams are digitized at 40 Msps which more then covers the 16 MHz analog band. The ADC is clocked with a 160 MHz clock which is locked to a local maser source. During the analog stage the RF, centered at 408 MHz, has been mixed down to baseband. Prior to digitization the last amplifier stage of the analog chain has per signal adjustable gain useful for setting good levels for ADC quantization. This ADC is connected via a dual Z-DOK interface to an 'F-Engine' ROACH which performs the channelization. The ROACH board is clocked at four times the sample rate such that four signals are time division multiplexed onto a single stream. Channelization is performed with a four tap Hann filter, 2048 point polyphase filterband (PFB) to produce 1024 samples per real antenna stream. The CASPER PFB has been modified to account for the signal multiplexing. Each channel has a width of 19.5 kHz and the output of th FFT stage is a 36 bit complex number. The narrow channel widths and PFB windowing allows for good frequency seperation in the high RFI environment at the observatory. After channelization the samples are quantized down to a 8 bit complex number. An adjustable, per channel complex gain equalizer is used for amplitude and phase corrections before quantization. Complex gain calibration is essential to proper spatial FFT imaging which must be applied before the spatial FFT. The FX correlator is used to generate calibration coefficents which are applied back into the equalizers. A selectable mux is available to skip the phase coefficents on the FX correlator data stream. Post equalization the data stream is split into two for specific reordering for the correlator and imager. The correlator data stream is reordered to 128 time samples for a single antenna for a single frequency channel. Followed by the next antenna and cycles back onto the next frequency channel. The imager takes in one time sample of each antenna for a given frequency channel

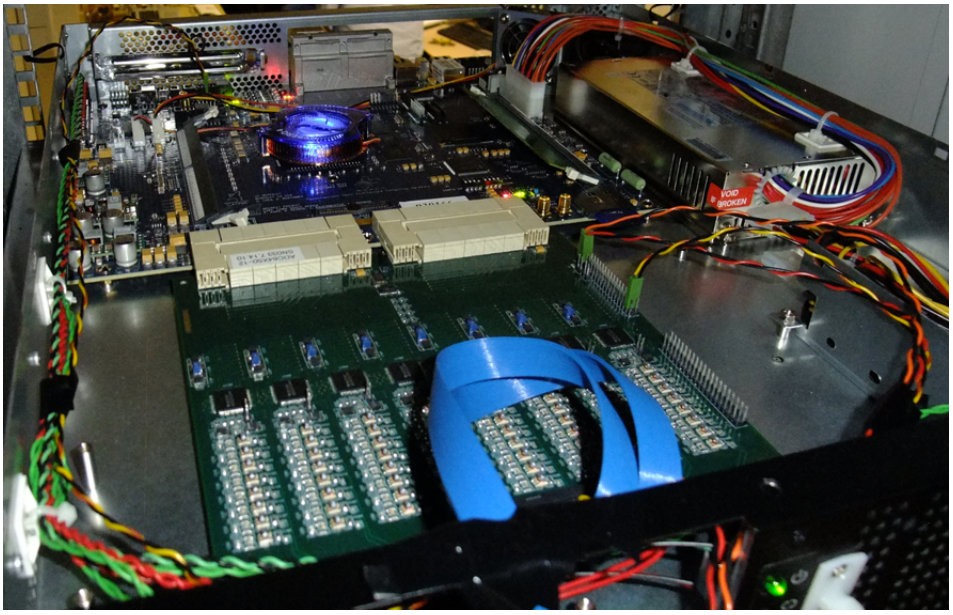

Figure 2. The 'f-engine' ROACH board, a Virtex 5 SX95T FPGA board, with the 64 input ADC connected via two Z-DOK connectors.

Digital Backend Specifications		
Digitizer/Channelizer (f-engine)		
Bandwidth	20	MHz
ADC Sampling	12	bit
Antenna-polarizations	32	single pol
PFB	4 tap 2048 point	
FFT	2048 point	Radix-2 Biplex Real
Quantization	4	bit
FX Correlator (x-engine)		
Auto Correlations	32	
Cross Correlations	496	
Minimum Integration Length	6.55	ms
Output	10 GbE	SPEAD protocol
Spatial FFT Imager (s-engine)		
2D FFT	8 x 16	
Beams	128	
Minimum Integration Length	1	s
Output	1 GbE	SPEAD protocol
Beamformer Output	10 GbE	Up to 8 Beams

Table 2. A three ROACH design where the correlator and spatial FFT imager use the digitizer/channelizer interface.

and cycles through 128 time samples before stepping to the next frequency channel. After data reordering each stream is sent over high speed XAUI at a rate of 5.12 Gbps to the correlator and imaging boards.

2.2 FX Correlator

An FX correlator design is a standard design for large bandwidth and many antenna arrays. The F component represents the frequency channalization, and the X is a complex multiply and accumulate (CMAC). An overview of the architecture is presented in (). Architecture efficency goes as $O(M\log M) + O(N^2)$ where M is the number of FFT frequency channels and N is the number of antenna-polarizations. The core component to the X stage of the FX correlator is the complex multiplication

F-Engine ROACH Resource Utilization (Virtex 5 SX95T)		
ADC Clock	40 MHz	
System Clock	160 MHz	Demux:4
Slice Registers	30217 / 58880	51%
Look Up Tables	24319 / 58880	41%
BRAM (36kb)	205 / 244	84%
DSP48e (Multipliers)	185 / 640	28%
CX-4 Interface	2 / 4	5.12 Gbps XAUI
QDR Memory	2 / 2	Cornerturn

Table 3. DSP implementation of the 'f-engine'

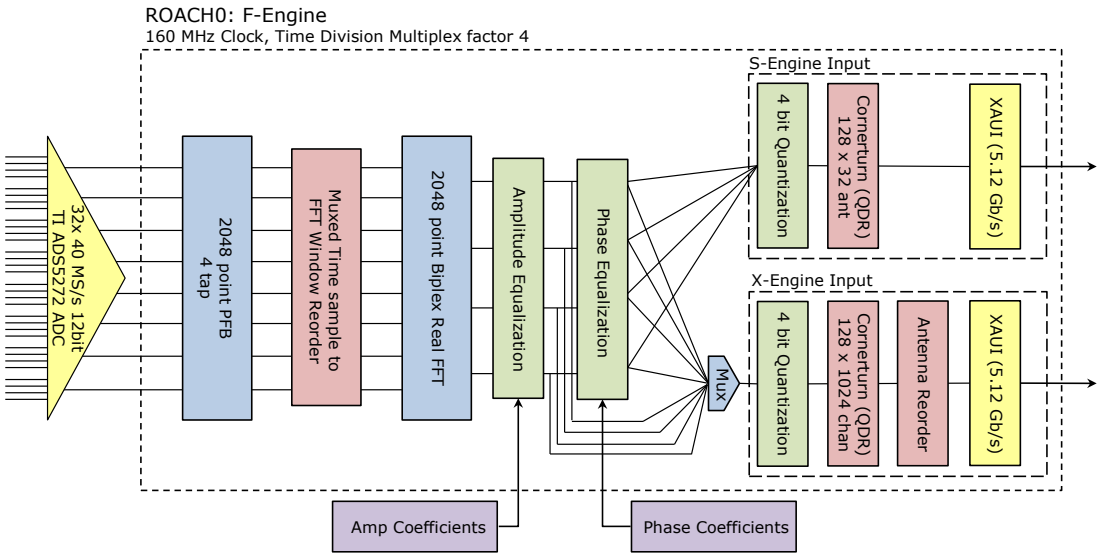

Figure 3. During observations amplitude and phase coefficents are applied to scale the power for the 4 bit correlation and apply phase corrections for the spatial FFT.

of all pairs of independent signals for each frequency channel. A pipelined x-engine, based on the general CASPER block originally designed by Lynn Urry(), is used for multiplier efficency. The pipeline design is constructed out of $M/2$ 'taps' where the i^{th} tap computes the correlation between antennas A_j and A_{j+i} for every antenna A_j of M total antennas. To maximize the multiplier usage a loopback is added to use every i^{th} tap to compute the correlation of antennas A_j and $A_{M/2+j+i}$, fig. 4. Each tap accumulates for N time samples to reduce the output data rate.

An asynchronous architecture is used between the f-enigne and x-engine boards. The x-engine board has been clocked

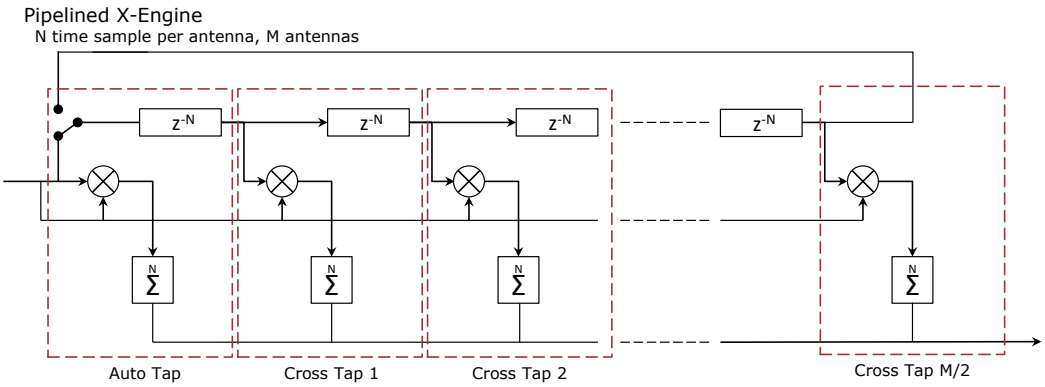

Figure 4. The input is ordered as N time samples per antenna per frequency channel. An accumulation stage after the complex multiply reduces the data rate of each tap. Outputs are multiplexed onto the same output using a valid signal.

X-Engine ROACH Resource Utilization (Virtex 5 SX95T)		
System Clock	200 MHz	
Slice Registers	28494 / 58880	48%
Look Up Tables	25349 / 58880	43%
BRAM (36kb)	88 / 244	36%
DSP48e (Multipliers)	288 / 640	45%
CX-4 Interface	1 / 4	5.12 Gbps XAUI
QDR Memory	2 / 2	Vector Accumulator

Table 4. DSP implementation of the 'x-engine'

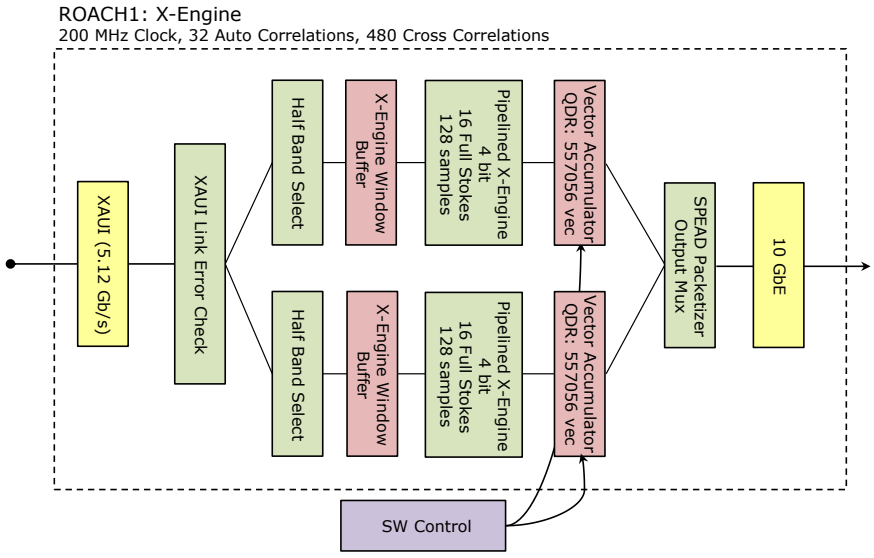

Figure 5. Two parallel pipelined x-engines are used, each processes half of the band.

to 200 MHz, well above the 160 MHz f-engine board, this assures the x-engine board will never have input buffer overflows during the windowing stage. The XAUI interboard connection is a streaming interface which garuntees the same output order as input order but with variable latency. In rare cases the XAUI interface can drop 64 bit words during the streaming, this requires an initial stage to track the number of words recieved between headers. In case of missing words the entire payload is dropped and counters reset for the next header. A correlation is only performed on a per channel basis. The channelized band can be split up into portions and processed in parrallel across multiple x-engines. This allows a larger bandwidth to be processed at the cost of increased logic and multiplier resource utilization. For this design two x-engines are used which each processes half of the band. The x-engine design requires a continuous stream of data for 128 samples of all antennas for a single frequency channel. Prior to the x-engine samples are buffered up into windows to garuntee valid data during a cycle of the x-engine. For reasons related to the design the 32 single polarization signals are treated as 16 dual polarization signals. This causes a small number of redundant baseline correlations and a conjugation effect which is corrected in post processing. During the x-engine stage an initial accumulation of 128 sample is performed after the complex multiply to reduce the output rate to roughly the input rate. This limits the minimum integration time to 6.55 ms. A vector accumulator using the on board QDR memory is used for longer integration lengths. This second accumulator is software controlled with integration lengths ranging from milliseconds to minutes. A completed integration is sent to a recieve computer over a 10 GbE connection. Integrations are split up based on the SPEAD protocol() and transmitted as UDP packets.

2.3 Spatial FFT

A spatial FFT imager is a novel instrument which takes advantage of the baseline redundancy in a regularly gridded array to reduce the correlator cost of an FX design $O(n^2)$ to a FFT cost of $O(n \log n)$. Correlation of all antenna pairs in a regularly gridded array makes redundant measurements for many of the baselines. This redundancy for the BEST-2 array is show in figure 10. Instead of making individual correlations of the same baseline as in an FX correlator the correlation of the average

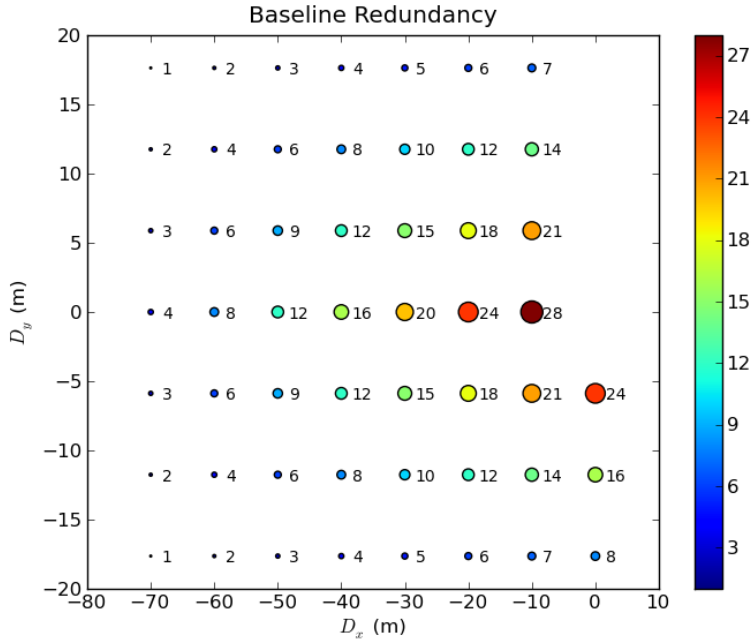

Figure 6. A 4 by 8 regularly gridded array has 52 unique baselines, 480 cross correlations are performed. The number of redundant baseline measurements is shown as the color and size of each circle.

of each baseline can be computed. This optimization realizes on the assumption that each redundant baseline measurement is indeed identical. Thus any calibration to the complex gains must be applied before the spatial FFT.

Though the X-Engine and S-Engine use the same F-Engine each requires a unique data windowing order. For the S-Engine a window is made up of N antennas by M time samples for a given frequency channel. A similar XAUI interface and windowing scheme is used as in the X-Engine which buffers up windows of valid data to stream into the spatial transform. The 2D spatial transform is performed using an 8 point FFT followed by a cornerturn and 16 point FFT. The BEST-2 array is a grid of 4 by 8 antennas, the data is zero padded before input into the 8 by 16 point spatial transform. A 4 by 8 point spatial transform will only produce gain information for each spatial position, which can be interpretted as an array of beamformers covering the field of view. This zero padding is necessary to produce both the gain and phase information of each spatial position which is an effective baseline. Each effective baseline is an average of all possible baselines with the same spatial dimensions. The four fold increase is the number of outputs from the spatial transform by double padding introduces a number of redundant calculations. The spatial transform produces 128 outputs, there are only 53 unique baselines in a 4 by 8 grid. The datarate out of the S-Engine is reduced by a two stage vector accumulator. A fixed 128 sample vector accumulator reduces the output of the second stage FFT so that the 1024 channels of the 128 computed spatial components can be multiplexed onto one line and accumulated in a software controllable QDR vector accumulator. Accumulations are sent out over the 1 GbE PowerPC interface using the a SPEAD UDP packet format. Individual beams can be selected out before accumulation and sent over 10 GbE in a LOFAR beam packet format which will be used for future pulsar processing.

3 DEPLOYMENT AND INITIAL OBSERVATIONS

Instrumentation was installed and tested over a two week period in April 2011. During that time a number of test signals were used to check the system status. Once the system was checked out various bright radio sources were obeserved. Since the Northern Cross is a transiting array there is a limited period of time each day in which a source is with the primary beam. Bright sources such as Cygnus A, Casseopia A and Virgo A also with a number of 3C sources were observed along with multiple constant declination 24 hour cycles were observed.

Raw data from the correlator and imager was recorded to HDF5 files using a SPEAD protocol receive script. A suite of python scripts have been written to interface and manipulate the data in this pre-calibration stage. A python FITS-IDI package has been written to convert HDF5 files into the standard FITS format which can be read by AIPS and CASA (). This allows for a trivial conversion to the Measurement Set format which most packages can interface with.

A number of calibration methods has been tested on the initial data sets. Traditional CASA based calibration has been used to form correlator images. To produce calibration coefficents for the spatial FFT imager a column ratio gain estimation

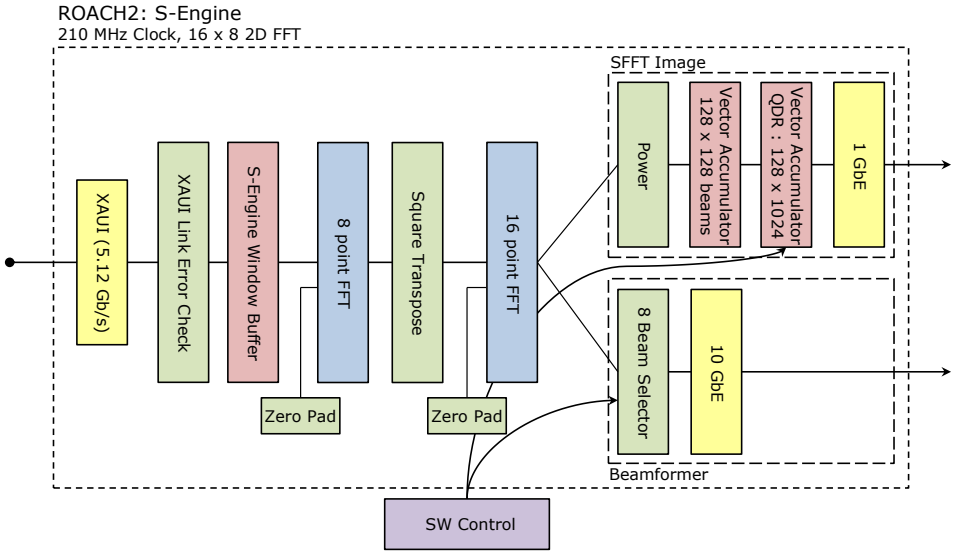

Figure 7. During the two stage spatial FFT the streams are zero padded to provide phase information of each baseline.

method has been employed. A study of the baseline redundancy and possible calibration has also been undertaken. Long observations of the sky are under way to understand the system noise and our ability to reach the confusion limit. During deep integration observations a cross talk issue covering part of the band has been discovered.

3.1 Calibration Methods

The effective averaging of redundant baselines in the spatial FFT imager requires complex gain calibrations to be applied during observations. To derive gain coeffiecents a calibration method is applied to the FX correlator data. In initial observations the column ratio gain esimation method from (Boonstra 2001) was used to compute a per channel, per antenna complex gain term.

3.2 FX Correlator Results

The East-West FWHM beam size of an individual element is 6.6° which translates to a 26 minute 'transit time' for an source. For the the bright A class sources this time can be extended since they remain the dominating source well after crossing the FWHM. Observations of 40-50 minutes are possible which gives an improvement in uv coverage. Initial calibration and imaging has been performed using the bright sources: Cygnus A, Cassiopeia A, Virgo A and Taurus A.

A transitting array provides a unique challenge of gain calibration since a source's apparent gain will change as it transits the primary beam. A typical beam transit of a strong source, Cygnus A, is show in figure **??**. The auto correlations asymmetry is due to the changing galactic plane pass through the beam. In the cross correlations the first and second sidelobes are evident. Much of the sky surrounding a bright source is contaminated due to these high sidelobes. The traditional method of using a gain calibrator is not possible. Gain calibration of bright sources was done by fitting a solution on short time intervals. A model of the beam will be necessary to set a better flux scale and time indepenedent gain solution.

Bright class A sources dominate the noise in a few seconds of integration. Images can be formed by taking short periods of time where the gain is effectively flat across the time interval.

Other sources, which are bright but a few orders of mangitude weaker than the class A sources have also been imaged. The bright 3C source 3C 196 can be imaged with 10's of seconds of integration. The flux scale on this source is off by a factor of approximately two because of our ability to set a flux scale based on a standard calibrator source and rely on a crude estamation using Cygnus A and Cassiopeia A.

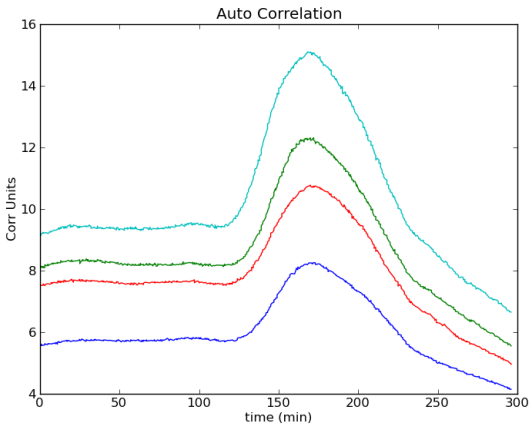

(a) A selection of typical auto correlations over a period of five hours during a transit of Cygnus A. The asymmetry is due to the background galactic plane.

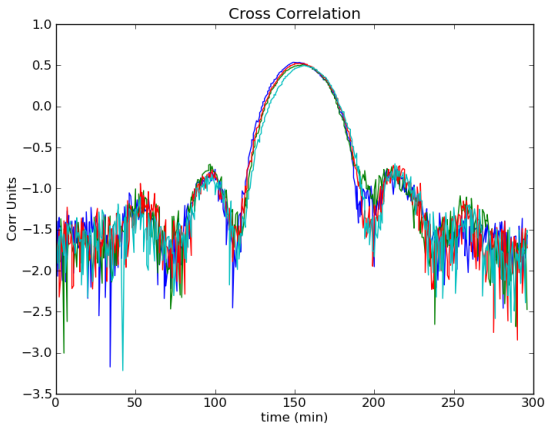

(b) Cross correlation power over a period of five hours during a Cygnus A transit. The first sidelobes are around 100 times lower then the primary lobe. A bright source like Cygnus A remains the dominant source in the field even into the second sidelobe.

Figure 8. Typical auto and cross correlations of a transiting source.

3.3 Spatial FFT Results

3.4 Comparison of FX Correlator and Spatial FFT

3.5 Crosstalk Effects

A strong cross talk effect has been observed in the lower portion of the band. This has the effect of creating a strong correlation, constant correlation across a few Megahertz before the effect tapers off below current noise measurements. Every baseline is affected to varying degrees, figure 11. The cross talk does not appear to be location or antenna dependent which suggests that it is not primarily from antenna coupling. A lab setup of the digital design has not been able to reproduce this effect but could still be related to the ADC cabling interface. Components with in the analogue chain could not be functioning within specification and causing the signal leakage. Further testing is required to discover the route of this issue.

3.6 Noise Floor Measurements

4 DISCUSSION

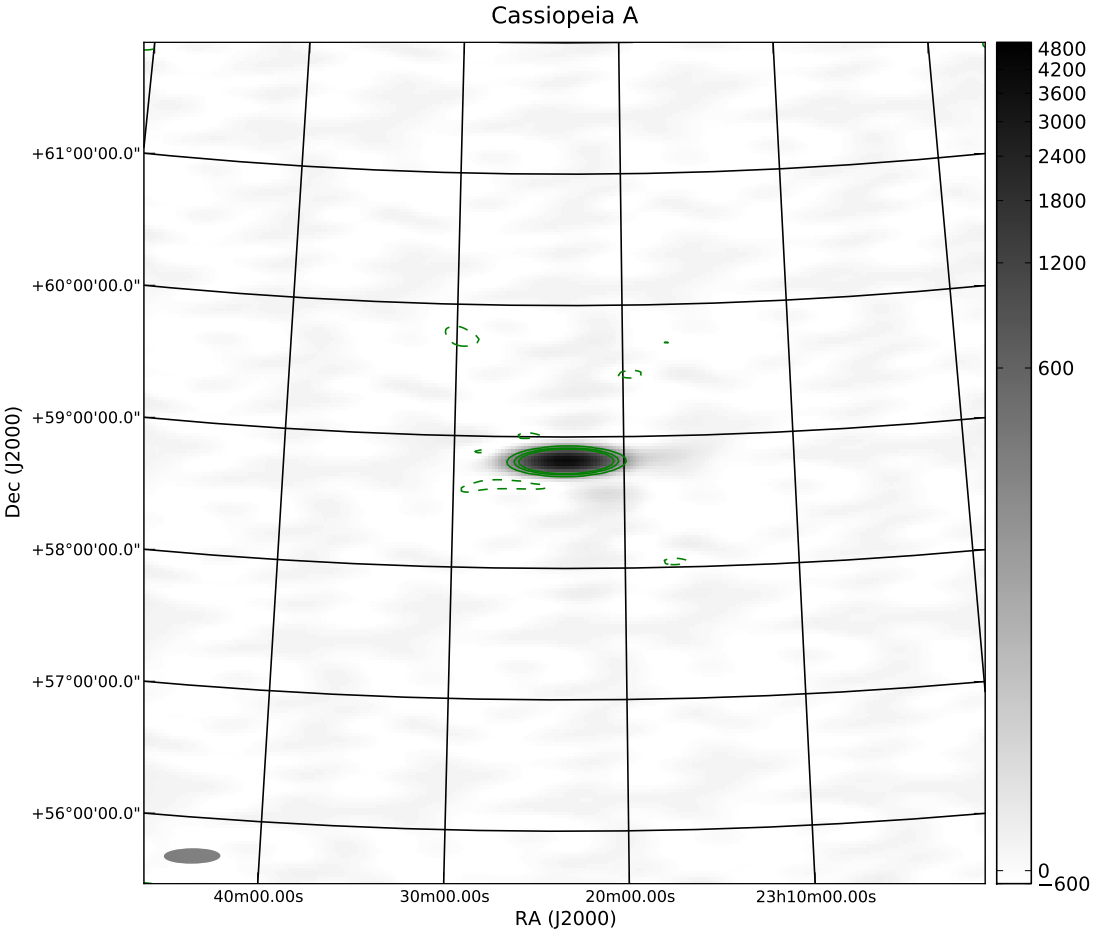

Figure 9. Calibrated image of Cassiopeia A using a 1 MHz portion of the band. This multi-frequency synthesis image was formed using a 40 minute transit of Cas A across the main lobe of the beam. The two 'sources' above and below the main source are artifacts of the first sidelobe. Beam effects are currently a limiting factor in improving the dynamic range of the image. The grayscale is Jy/Beam, with a nominal noise floor of ≈ 10 Jy.

REFERENCES

A.J. Boonstra and A.J. Van der Veen, "Gain Decomposition Methods for Radio Telescope Arrays", 2001 *IEEE Workshop on Statistical Signal Processing (SSP)*, Singapore, August 2001

S. Montebugnoli, G. Bianchi, J. Monari, G. Naldi, F. Perini, and M. Schiaffino, "BEST: Basic Element for SKA Training", 2009 *SKADS Conference 2009: Widefield Science and Technology for the SKA*, p. 331-336

S. Montebugnoli, M. Bartolini, G. Bianchi, G. Naldi, J. Manley, and A. Parsons, "BEST Back End", 2009 *SKADS Conference 2009: Widefield Science and Technology for the SKA*, p. 355-358

E. Otobe, J. Nakajima, K. Nishibori, T. Saito, H. Kobayashi, N. Tanaka, N. Watanabe, Y. Aramaki, T. Hoshikawa, K. Asuma, and T. Daishido, "Two-dimensional Direct Images with a Spatial FFT Interferometer", 1994, *PASJ*, Vol. 46, No. 5, p. 503-510

F. Perini, G. Bianchi, M. Schiaffino, and J. Monari, "BEST Receiver Experience: General Architecture, Design and Integration", 2009 *SKADS Conference 2009: Widefield Science and Technology for the SKA*, p. 351-354

F. Perini, "Low Noise Design Experience for the SKADS/BEST Demonstrator", 2009 *SKADS Conference 2009: Widefield Science and Technology for the SKA*, p. 341-345

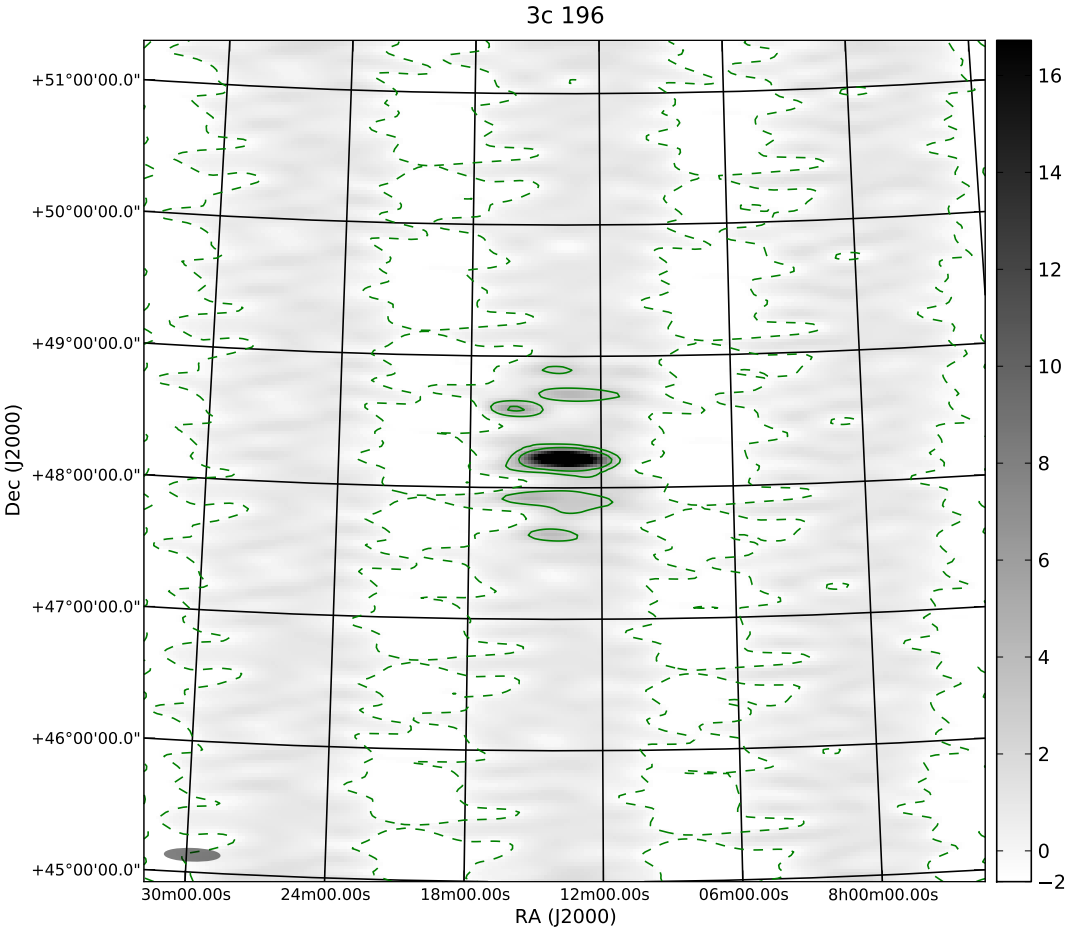
3c 196
+51°00'00.0"
+50°00'00.0"
+49°00'00.0"
+48°00'00.0"
+47°00'00.0"
+46°00'00.0"
+45°00'00.0"
Dec (J2000)
30m00.00s
24m00.00s
18m00.00s
12m00.00s
06m00.00s
8h00m00.00s
RA (J2000)
16
14
12
10
8
6
4
2
0
−2

Figure 10.

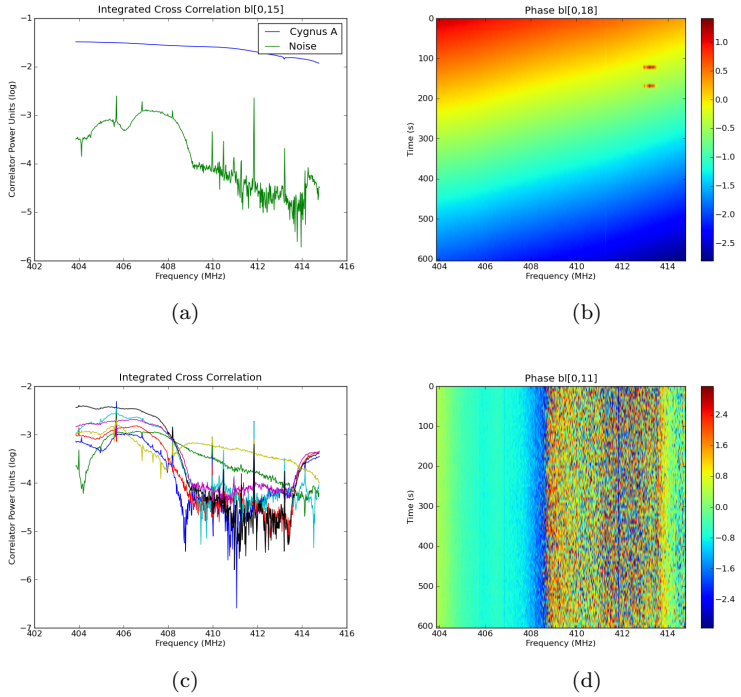

Figure 11. The lower portion of the band has a strong correlation effect caused by cross talk. On observing strong sources the effect is weak but becomes a dominate effect when observing a cold patch of the sky, fig. 11a. Cross talk is noticable in almost all the cross correlations, fig. 11c shows a handful of baselines. This effect is difficult to localize, there is no obvious systematic effects with regard to antenna locations or cabling. Figure 11b is a phase plot (Radians) of the observation of bright source. Figure 11d is a phase plot of a region with no sources, the cross talk has the effect of flattening the lower end of the band.